International Journal of Engineering

Journal Homepage: www.ije.ir

An Experimental Study to Predict a New Formula for Calculating the Deflection in Wide Concrete Beams Reinforced with Shear Steel Plates

A. S. Mohammed[a], A. S. J. Al-Zuheriy*[a], B. F. Abdulkareem[b]

[a] *Civil Engineering Department, University of Technology – Iraq, Baghdad, Iraq*
[b] *Civil Engineering Department, Al-Mansour University College, Baghdad, Iraq*

PAPER INFO

Paper history:
Received 10 October 2022
Received in revised form 27 October 2022
Accepted 28 October 2022

Keywords:
Moment of Inertia
Shear Failure
Stirrups
Beams Strengthening

ABSTRACT

A conventional stirrup is widely used in all concrete beams as shear reinforcement to prevent shear failure that happens suddenly and unexpectedly without previous warning. It is a great challenge to figure out another type of stirrup and establish a new formula to calculate the deflection. This article offers an experimental study that predicts a novel formula for calculating deflection in concrete beams reinforced with shear steel plates as a stirrup. The experimental work was established and consists of 16 wide reinforced concrete beams with 216x560x1800 mm dimensions. Instead of the conventional reinforcing stirrups, steel plates with 3.0, 4.0, and 5.0 mm thickness in longitudinal and transverse dimensions and for one-half of the samples, recycled PVC round bubbles were used as the variables explored in this study. In addition, the variables include an examination of the opening form of shear steel plates with varying distances between them. For calculating the deflection of wide beams, a new formula for the effective moment of inertia is proposed, and it yields excellent agreement for several investigations, with a coefficient of variation of 5.48 percent. The formulae for calculating the maximum deflection are established using ACI 318M-14 and EC 2.

***doi**: 10.5829/ije.2023.36.02b.15*

1. INTRODUCTION

In recent years, the use of large concrete beams in structural framing systems has increased. This modification addresses the need for low-cost keys that minimize the structural height and architectural complexity. Broad beams may offer enough cross-sectional areas to perform the needed function at a shorter depth than a system of narrower beams with parallel spacing in the plan; when coupled with reinforced concrete broad beam-column connections. It is very effective at resisting earthquake stresses.

Sherwood et al. [1] conducted an experimental investigation to determine the shear behavior of broad beams and thick slabs, as well as the effect of element width. In their investigation, they examined five specimens of standard-strength concrete ranging in width from 250 to 3005 mm and nominal thickness from 470 mm. Their research revealed that the shear failure stresses of narrow beams and broad beams are very comparable.

Adam et al. [2] studied the effect of shear reinforcement spacing on the unidirectional shear capacity of broad reinforced concrete components. A set of thirteen concrete examples of typical strength were constructed and tested. The spacing of shear reinforcements was the key test variable. The specimens' shear reinforcement ratios were in close proximity to ACI 318-11 [3] minimum standards. To ensure that the shear strength of all elements with shear reinforcement produced in accordance with ACI 318-11 is adequate. The study advises restricting the transverse spacing of web reinforcement to the lesser of the effective element depth or 600 mm.

Hanafy [4] noted that the test findings show the relevance of web reinforcement in strengthening the shear capacity and ductility of narrow broad beams, which conform to globally recognized norms and standards.

*Corresponding Author's Email: ahmed.sh.jeber@uotechnology.edu.iq (A. S. J. Al-Zuheriy)

Please cite this article as: A. S. Mohammed, A. S. J. Al-Zuheriy, B. F. Abdulkareem, Experimental Study to Predict a New Formula Calculating the Deflection in Wide Concrete Beams Reinforced with Shear Steel Plates ***International Journal of Engineering, Transactions B: Applications***, Vol. 36, No. 02, (2023), 360-371

The deflection, strain, and fracture patterns of four examined full-scale reinforced concrete beams are estimated using theoretical and experimental analysis in this paper. Said and Elrakib [5] examined the shear behavior of broad beams. The testing program had 9 beams of 29.0 MPa concrete strength, each measuring 700.0 mm in width, 250.0 mm in depth, and 1750.0 mm in length, with a 650 mm shear span. The research demonstrates that the contributions of stirrups to shear strength are substantial and directly related to the quantity and spacing of stirrups. Compared to the reference beam, the maximum shear stress of the range of tested beams increased by between 32% and 132%. Broad beams' shear resistance was more effectively contributed to by high-grade steel.

Mohammadyan-Yasouj et al. [6] studied six broad beams with inner column specimens, one sample for each of the following conditions: without web reinforcement, with web reinforcement. According to the findings, independent bent bars enhanced the shear capacity and ductility of broad beams. Although independent strait bars enhanced the shear strength to some degree, it was determined that the beam was less ductile upon failure. In addition, the findings revealed that the beam with banded primary longitudinal reinforcement attained a higher failure load.

The risk management and earthquake research and applications center [7] showed a new technology. An experimental evaluation of reinforced concrete broad beams strengthened with lattice girders, commonly known as one-way slabs, are subjected to low-rate (static) concentrated loads at their midspan. To determine the impact of lattice girders on load-bearing capability, tests were performed on lattice girder-reinforced and conventionally reinforced beam-type specimens. Six beams with two distinct reinforcing configurations were evaluated. The examined beams were supported by a simple 2250.0 mm span. All specimens were subjected to static loading tests, and mid-span deflections were measured using displacement transducers. The lattice girder-reinforced and conventionally reinforced beams exhibited comparable stiffness, while the lattice girder-reinforced beams exhibited a better resisting capacity.

Ibrahim et al. [8] investigated the strength of bubbling broad reinforced concrete beams with various shear steel plate kinds. A total of eight specimens were examined. The factors examined concern the replacement of stirrups with shear steel plates of the comparable cross-sectional area for stirrups at mid-leg height with circular openings of varying thicknesses (3, 4, and 5 mm). Four specimens lacked bubbles, whereas the remaining specimens included bubbles. This research revealed that shear steel plates are a viable replacement for stirrups; since they increased yield, ultimate load, and deflection (at service load) by an average of 5%, 15%, and 9% as compared to utilizing bubbles. The yield deflection is enhanced by 24%, 37%, and 27% for 3, 4, and 5mm thick shear steel plates, respectively, as compared to 10mm stirrups, and it was within 8% for all samples when utilizing bubbles.

Eklou et al. [9] looked at how steel plate pieces and regular stirrups worked as shear reinforcement in beams. In this experiment, two full-size reinforced concrete beams were made to fail in shear. The types of shear reinforcement were used as the test parameters for this study. By looking at the crack configurations, load-deflection relationship, and shear capacities of the samples, the shear resistance of the beams was discussed. The values predicted by the Modified Truss Theory were compared to the shear capacities that were found through experiments. The proportion of the evaluated shear strength to the predicted shear capacity in the steel plate RC beams and the reference beam showed that they were pretty close. The findings of this research demonstrate that the global behavior of the steel plate beam and the control beam using traditional stirrups is only slightly different.

Hamoda et al. [10] look into how engineered cement composite (ECCO) and stainless steel plates can make concrete members stronger. For samples strengthened with an ECCO layer, non-linear 3D finite element models were made. When the lab tests were compared to the model, it was discovered to be accurate. Depending on the results of the experiments and the numeracy data, new shear strength formulas were made.

Due to the importance of shear failure in reinforced concrete members which is happened suddenly without warning, Alferjani et al. [11] and Abdollahi et al. [12] presented the experimental and analytical studies for reinforced concrete members to evaluate the shear capacity. Rahmani et al. [13], Faez et al. [14] and Mohsenzadeh et al. [15] studied the reinforced concrete beams strengthening due to the importance of this topic.

Aydin et al. [16] investigated the various effects of using steel diagonal elements and dampers as strengthening materials on the structural responses as well as the best placement locations in terms of different structural response parameters. They found that both viscous dampers and steel diagonal braces reduce the top story displacement.

Aydin et al. [17] showed the concepts and the principles of using the steel plate systems and studied the effects of steel plates on 5-story and 10-story steel buildings to strengthen frames.

The novelty of this work is to predict a novel formula for calculating deflection in concrete beams reinforced with shear steel plates as a stirrup. The objectives of this research are represented by offering an experimental study that included testing 16 concrete beams with 33.0 MPa as nominal compressive strength under the four-point loading test with studied different variables consist steel plates with 3.0, 4.0, and 5.0 mm thickness in longitudinal and transverse dimensions, instead of the conventional reinforcing stirrups and for one-half of the samples, recycled PVC round bubbles. In addition, the variables

include an examination of the opening form of shear steel plates with varying distances between them.

In this study, the main goal of the study is to find a new way to figure out how much W-reinforced concrete (RC) beams with steel shear plates bend and to predict the new equation to estimate the deflections in these types of beams. In fact, using a steel plate is a new way to deal with a lot of stirrups in a broad (RC) beam because concrete's shear portion is very tiny when compared to high-depth concrete beams.

2. EXPERIMENTAL TEST DETAILS

The experimental work included testing 16 concrete beams with 33.0 MPa as nominal compressive strength (SCC - Self Compacting Concrete) under the four-point loading test. All of the samples had a width of 560mm and a height of 216mm. The beam's effective depth is 170mm. All of the beams were made stronger by adding 10 ø 16.0 mm bars in tension and 2 ø 10.0 mm bars in the compression zone. This steel ratio is greater than the minimum and larger than the maximum ratios that the ACI M-318-14 says should be used [3]. In the middle of the beam, there were no stirrups. Table 1 shows details and notes about each of the sixteen beam specimens. The last number, -1, -2, or -3, tells you how far apart the steel plates are: 125 mm, 166 mm, or 250 mm. The symbol shows the diameter of the steel bars that run lengthwise.

Figure 1 shows the typical sizes and details of the reinforcing bars of the specimens that were tested. Figures 2 and 3 show cross-sections of the same specimens. Figure 4 shows where the bubbles go, and Figure 5 shows where the longitudinal main reinforcement and the steel shear plate are located.

3. RESULTS AND DISCUSSION

3. 1. Result of Beam Specimens Table 2 lists the f'_c, cracks, yielding stress, ultimate loads, deflections at the crack, and ultimate loading, as well as the ductility factor for each specimen. The load at which the first crack appeared was carefully noted. Load-deflection graphs were used to figure out the experimental results of the cracking loads.

TABLE 1. Specimens' details

Beam Name	B * H (mm)	a /d	Reinforcing of main Bars		Shear Rein.	Plate thicknesses (mm)	Spacings (mm)	Bubbles Diam. (mm)
			Ten.	Comp.				
BWS	560x216	3.529	10 ϕ 16.0	2 ϕ 10.0	Double stirrups ϕ 10	---	125.0	--
BWBS	560x216	3.529	10 ϕ 16.0	2 ϕ 10.0	Double stirrups ϕ 10	---	125.0	85.0
BWP3-1	560x216	3.529	10 ϕ 16.0	2 ϕ 10.0	--	3.0	125.0	--
BWBP3-1	560x216	3.529	10 ϕ 16.0	2 ϕ 10.0	--	3.0	125.0	85.0
BWP3-2	560x216	3.529	10 ϕ 16.0	2 ϕ 10.0	--	3.0	167.0	--
BWBP3-2	560x216	3.529	10 ϕ 16.0	2 ϕ 10.0	--	3.0	167.0	85.0
BWP3-3	560x216	3.529	10 ϕ 16.0	2 ϕ 10.0	--	3.0	250.0	--
BWBP3-3	560x216	3.529	10 ϕ 16.0	2 ϕ 10.0	--	3.0	250.0	85.0
BWP4	560x216	3.529	10 ϕ 16.0	2 ϕ 10.0	--	4.0	125.0	--
BWBP4	560x216	3.529	10 ϕ 16.0	2 ϕ 10.0	--	4.0	125.0	85.0
BWP5	560x216	3.529	10 ϕ 16.0	2 ϕ 10.0	--	5.0	125.0	--
BWBP5	560x216	3.529	10 ϕ 16.0	2 ϕ 10.0	--	5.0	125.0	85.0
BWPR4	560x216	3.529	10 ϕ 16.0	2 ϕ 10.0	--	4.0	125.0	--
BWBPR4	560x216	3.529	10 ϕ 16.0	2 ϕ 10.0	--	4.0	125.0	85.0
BWPL3	560x216	3.529	10 ϕ 16.0	2 ϕ 10.0	--	--	--	--
BWBPL3	560x216	3.529	10 ϕ 16.0	2 ϕ 10.0	--	--	--	85.0

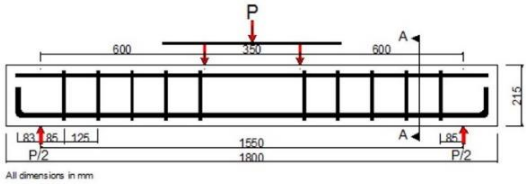

Figure 1. Loading details

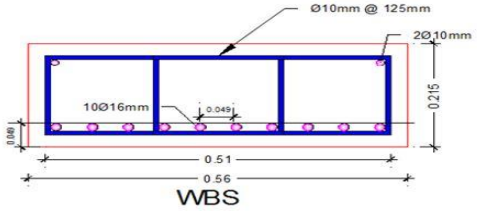

Figure 2. Section A-A stirrups (BWS beam)

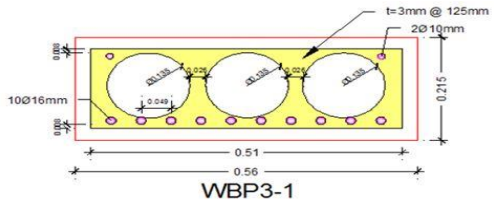

Figure 3. Section A-A for plates (BWP3-1 beam)

Figure 4. Preparation of the molded specimen and placing the reinforcement

Figure 5. Preparation and lying the bubles on the right side of the specimen

TABLE 2. The examined specimens' strength characteristics

Beam Name	Compressive Strength f'_c (MPa)	Measured Cracking load P(kN)	Measured Δ_{cr} (mm)	Yielding load P(kN)	Measured Δ_y (mm)	Ultimate Load P (kN)	Measured Δ_u (mm)	Ductility= $\frac{\Delta_u}{\Delta_y}$	Failure mode
BWS	36.60	50.0	1.730	400.0	10.830	440.0	18.930	1.750	Flexural
BWBS	33.20	40.0	1.500	361.0	13.400	378.0	25.700	1.920	Flexural
BWP3-1	33.50	50.0	1.530	420.0	13.450	431.0	36.450	2.710	Flexural
BWBP3-1	33.10	60.0	2.100	421.0	12.30	446.0	22.500	1.830	Flexural
BWP3-2	34.00	60.0	2.900	400.0	13.150	441.0	23.100	1.760	Flexural
BWBP3-2	32.50	50.0	2.100	410.0	16.850	430.0	35.750	2.120	Flexural
BWP3-3	32.80	40.0	1.760	370.0	11.330	376.0	22.820	2.010	Shear
BWBP3-3	32.90	40.0	1.750	410.0	14.800	431.0	28.600	1.930	Shear
BWP4	32.40	50.0	2.050	420.0	14.550	441.0	30.350	2.090	Flexural
BWBP4	32.60	50.0	1.900	420.0	14.080	441.0	21.280	1.510	Flexural
BWP5	32.40	50.0	1.900	410.0	13.750	419.0	17.750	1.290	Flexural
BWBP5	33.40	50.0	2.130	410.0	13.750	431.0	20.050	1.460	Flexural
BWPR4	33.20	50.0	2.250	370.0	13.000	380.0	17.600	1.350	Flexural
BWBPR4	32.60	50.0	2.200	400.0	15.900	420.0	18.900	1.190	Flexural
BWPL3	32.320	40.0	2.350	400.0	11.350	450.0	22.450	1.980	Flexural
BWBPL3	32.80	80.0	2.800	400.0	14.050	431.0	25.250	1.800	Flexural

3. 2. The Deflection Comparison Computed by ACI 318-14 and EC 2 Codes The experimental deflection computed from load-deflection curves at service load which is assumed 60.0 % of the ultimate loads and the analytical deflection outcomes at service load of all specimens computed by ACI-318-14 [3] codes are presented in Table 3. It can be noticed that the analytical deflections of wide beams computed by ACI-318-14 [3] codes were on average 24% and 25% lower than the experimental deflection, respectively. This increase in experimental deflection is due to the ability of the dial gauge to catch the readings of deflection at the center of wide beams in both directions (longitude and transverse) while the dial gauge cannot catch the readings of deflection at the edges of the center of the beam.

By Saint-Venant's principle, this case makes sense. Saint-Venant's theorem says that when a system of forces is imposed on a small part of a body's boundary, the stresses and strains caused by such forces in that other part of the body, which is far away from the region where the forces are applied, do not depend on how the forces are implemented, but only on what happens as a result. Most of the time, this huge distance can be thought of as the largest dimension of the area where the forces are implemented [18].

Take the prismatic bar shown in Figure 6 as an example. The stresses at a length farther than the transverse dimension (2*b) from the top of the steel bar can be considered equal in all three cases when three systems of forces have the same effect.

TABLE 3. Experimental deflections compared with deflections computed by ACI 318-14 [18] codes at service load

Beam Name	Deflections at Service Load, Δ_s (mm)				
	Measured	Predicted			
		ACI-318M-14		EC-2	
			%Differences		%Differences
BWS	3.50	3.010	-13.930	3.000	-14.260
BWBS	3.60	2.6000	-27.640	2.600	-27.520
BWP3-1	3.10	2.9600	-4.2840	2.9640	-4.3740
BWBP3-1	3.70	3.070	-16.810	3.070	-16.870
BWP3-2	4.40	3.000	-31.700	3.000	-31.660
BWBP3-2	4.50	3.000	-33.270	3.000	-33.270
BWP3-3	3.60	2.610	-27.290	2.610	-27.340
BWBP3-3	4.10	3.000	-26.700	2.990	-26.840
BWP4	4.10	3.040	-25.840	3.040	-25.710
BWBP4	4.00	3.070	-23.170	3.060	-23.280
BWP5	3.60	2.920	-19.960	2.920	-19.990
BWBP5	4.20	2.960	-29.430	2.960	-29.420
BWPR4	4.10	2.590	-36.710	2.590	-36.580
BWBPR4	4.30	2.900	-32.370	2.900	-32.380
BWPL3	4.10	3.180	-22.350	3.170	-22.510
BWBPL3	4.00	3.010	-24.740	3.000	-24.830

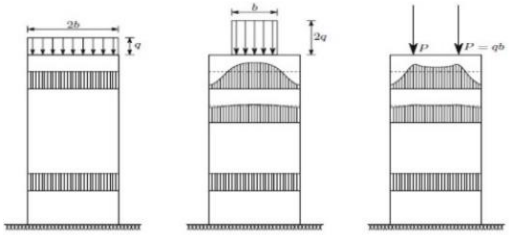

Figure 6. The distributions of stree due to three force systems with the same resultant for several bar cross-sections [3]

3. 3. Deflection Suggestion Models The cracked and uncracked section characteristics of the tested beams were used to look at the deflections of the flexural tests. The goal was to come up with a system design for checking the deflection of a broad beam under the effect of service load. The following equations were given by ACI-318-14 [3] codes to figure out the maximum deflection.

3. 3. 1. Deflection Calculation According to ACI 318M-14 By adding up the curves along the length

of a beam, you can figure out how it will bend. For an elastic beam, the curvature, 1/r, is equal to M/EI, where (EI) is the stiffness of the flexural member of the cross-section. If EI stays the same, this is a normal thing to do. But three different EI values should be thought about for reinforced concrete. Figure 7 shows moment-curvature diagrams for a beam with many cracks. The following diagram shows how these things work [19]. The uncracked inertia moment EI_u refers to the moment of inertia of any section before it cracks. And the radial O-A in Figure 7 shows how the conformable EI_u works. After a crack happens, the section's inertia moment is called the "cracked moment of inertia," EI_{cr}, and it is smaller than the uncracked moment of inertia. There are intermediate values of EI between where the steel breaks (point A) and where it gives way (point B).

The transition from I_{gt} to I_{cr} that is noticed in the experimental data was derived in the following equation by James et al. [19]:

$$I_e = \left(\left(\frac{M_{cr}}{M_a}\right)^3 I_g\right) + \left(1 - \left(\frac{M_{cr}}{M_a}\right)^3\right) I_{cr} \quad (1)$$

In Figure 8, the four-point-loaded beam deflection was predicted using the formula given in Equation (2):

$$\Delta_{max} = \left(\frac{Pa\left(3L^3 - 4a^2\right)}{48 E_c I_{effective}}\right) \quad (2)$$

where L is the beam length, P is the applied load, E is the elastic modulus, and a is the length between the point load and the beam's edge.

3. 3. 2. Deflection Calculation According to EC 2 Model An equation was used to figure out how much a structure bends; this equation was used by EC 2.

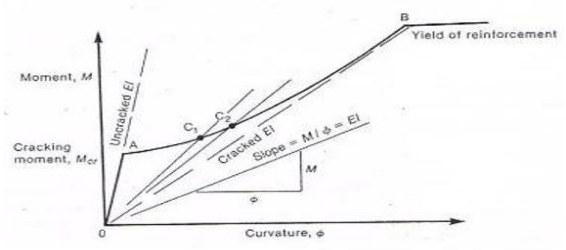

Figure 7. Moment-curvature diagram

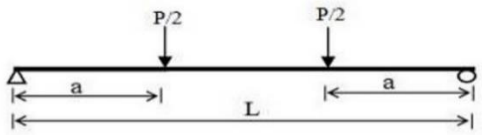

Figure 8. Testing set up

$$M_{cr} = \frac{0.9 f_{ctm} \cdot I_u}{h - x_u} \quad (3)$$

where f_{ctm} is the rupture modulus, I_u is the inertia moment of gross sectional area, h is the height of the sample, and x_u is the distance of the level of the uncracked section neutral axis from the tension face.

$$\xi = 1 - 0.5\left(\frac{M_{cr}}{M_a}\right)^2 \quad (4)$$

$$\frac{1}{r_n} = \xi\left(\frac{M_{QP}}{EI_c}\right) + (1 - \xi)\left(\frac{M_{QP}}{EI_u}\right) \quad (5)$$

$$\frac{1}{r_{t,QP}} = \left(\frac{1}{r_n}\right) + \left(\frac{1}{r_{cs}}\right) \ (i.e\ \Phi) \quad (6)$$

$$\delta_{QP} = kl^2 \frac{1}{r_{t,QP}} \quad (7)$$

$$k = \left(0.125 - \frac{(a/l)^2}{6}\right) \quad (8)$$

3. 3. 3. Modified Stiffness Equation for Wide Beams In the preceding section, it was made clear that the equations used do not ensure a good job of predicting deflection for broad beams. So, a new equation is needed to anticipate how much the beam will bend. The moment of inertia that works I_e is the most important factor in figuring out how much beams bend. By applying the displacement equation based on the structural analysis and the elastic bending theory, the next method is according to an analysis of all the information about displacement readings at mid-span. Equation (9) is used to calculate the bending stiffness.

$$E_c I_{effective} = \left(\frac{Pa(3L^2 - 4a^2)}{48\ \Delta_{max}}\right) \quad (9)$$

Where: Δ_{max} represents the experimental deflection value. Upon removing the service load (approximately 250 kN). It is possible that the increased experimental deflection and reduced stiffness of the broad beam are because the deflection at the end of the transverse direction is smaller than at the center point of the beam according to the Sant Venant principle. Bending stiffness may also be measured in terms of curvature, as shown in Figure 9 and represented by Equation (10).

In Figure 9, the values of ε_c, ε_s, k_d, and d-k_d are compression concrete strains in the top fiber, tensile steel strains, depth of the neutral axis at the service stage, and depth of the neutral axis at the ultimate stage, respectively.

$$E\ I_{exp} = \frac{M}{\Phi} \quad (10)$$

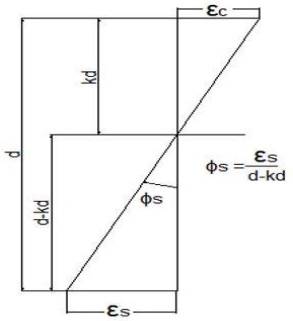

Figure 9. service-curvature (φy) in bending sections

With Equation (11) and the strain in concrete and steel measured during loading, we can calculate the curvature.

$$\Phi = \frac{\varepsilon_s}{d - kd} \tag{11}$$

Table 4 describes the $I_{\exp}$ values calculated by Equation (10) that were based on the $M_{service}$ equals 60.0 % of $M_{ultimate}$ and curvatures Φ that are based on the experimental strain of longitudinal bars and depth of neutral axis on the service load state. Also, Table 4 demonstrates the $I_{\exp}$ values calculated by Equation (9) based on the experimental deflection at the service state.

The difference in average between Equation (10)'s EI_{exp} and Equation (9)'s EI_{eff} value was 1.50 %, so the two values were very close to each other. In this paper, the values of curvature were used to figure out the effective inertia moment.

Tables 5 and 6 show how the effective moment of inertia from Equation (10) compares to the completely dependent deflection at the service stage from ACI-318-14 [3]. It is obvious that 138.6% and 138.26% were the difference in the average of (I_{exp} / I_{eff}) for ACI 318M-14 [3] and for EC 2, respectively. As well, -74.07% and -74.12% were the average deflection differences for ACI 318M-14 [3] and -73.96% for EC 2, respectively.

To determine the deflection and the ductility index, load section stiffness and load-neutral axis depth diagrams were used by Mohammad [20]. Then according to ACI 318M-14 [3] and EC 2 for wide beams, a new equation (Equation (12)) was modified to predict the deflection depending on the experimental stiffness values and the experimental curvature values calculated from Equations (9) and (10), respectively.

$$I_e = 0.740\left(\left((\frac{M_{cr}}{M_a})^3 I_g\right) + \left(1 - (\frac{M_{cr}}{M_a})^3\right) I_{cr}\right) \tag{12}$$

At the service load, the deflection results computed by the modified Equation (12) compared with the experimental deflection are shown in Table 7. It was obvious that the difference between the actual deflection and what ACI-318-14 [3] and EC 2 calculated was 1.40 % and 1.30 %, respectively.

TABLE 4. Bending and curvature stiffness Equations (10) and (11)

Beam Name	From Equation (10)				From Equation (11)		$\frac{EI_{effective}}{EI_{\exp}}$ %
	ε_s	(d-kd) mm	Φ x10^{-5} (mm^{-1})	$M_{service}$ (kN.m)	$EI_{\exp}$ (x10^{12})	$EI_{effective}$ (x10^{12})	
BWS	0.00150	110.0	1.3630	79.200	5.8080	5.4360	93.6010
BWBS	0.00160	104.0	1.5380	68.040	4.4230	4.5410	102.670
BWP3-1	0.00130	112.0	1.1600	77.580	6.6840	6.0120	89.9550
BWBP3-1	0.00160	108.0	1.4810	80.280	5.4190	5.2130	96.2000
BWP3-2	0.00180	92.0	1.9560	79.380	4.0570	4.3340	106.840
BWBP3-2	0.00180	87.0	2.0680	77.400	3.7410	4.1320	110.470
BWP3-3	0.00140	87.0	1.6090	67.680	4.2060	4.5160	107.390
BWBP3-3	0.00150	88.0	1.7040	77.580	4.5510	4.5460	99.8900
BWP4	0.00160	95.0	1.6840	79.380	4.7130	4.6510	98.6990
BWBP4	0.00150	90.0	1.6660	79.380	4.7630	4.7680	100.110
BWP5	0.00150	98.0	1.5300	75.420	4.9270	4.9640	100.750
BWBP5	0.00170	95.0	1.7890	77.580	4.3350	4.4380	102.370
BWPR4	0.00180	94.0	1.9140	68.400	3.5720	4.0080	112.210
BWBPR4	0.00170	87.0	1.9540	75.600	3.8690	4.2240	109.180
BWPL3	0.00160	97.0	1.6490	81.000	4.9110	4.7460	96.6640
BWBPL3	0.00140	87.0	1.6000	77.580	4.8210	4.6600	96.6600
C.O.V.							1.50 %

TABLE 5. The comparison of Equation (10) with ACI-318-14 [3] at the service stage for the moment of inertia and deflection

Beam Name	From Equation (10)		From Equation (2)		I_{exp}/I_{eff} (%)	$\frac{\Delta_{s(equation2)}}{\Delta_{s(equation10)}}$ (%)
	I_{exp} x10^8	Δ_s (mm)	$I_{eff.}$ x10^8	Δ_s (mm)		
BWS	1.85	3.310	2.046	3.01	110.59	90.936
BWBS	1.51	3.731	2.178	2.60	144.23	69.686
BWP3-1	2.22	2.823	2.111	2.96	95.090	104.85
BWBP3-1	1.81	3.594	2.126	3.07	117.45	85.420
BWP3-2	1.28	4.735	2.038	3.00	159.21	63.357
BWBP3-2	1.34	5.005	2.253	3.00	168.13	59.940
BWP3-3	1.50	3.901	2.246	2.61	149.73	66.905
BWBP3-3	1.60	4.130	2.216	3.00	138.50	72.639
BWP4	1.59	4.081	2.143	3.04	134.77	74.491
BWBP4	1.67	4.039	2.210	3.07	132.33	76.008
BWP5	1.75	3.712	2.236	2.92	127.77	78.663
BWBP5	1.43	4.334	2.112	2.96	147.69	68.297
BWPR4	1.16	4.635	2.099	2.59	180.94	55.879
BWBPR4	1.32	4.729	2.172	2.90	164.54	61.323
BWPL3	1.87	3.997	2.365	3.18	126.47	79.559
BWBPL3	1.85	3.901	2.241	3.01	121.13	77.159
COV					+138.6%	-74.07%

TABLE 6. The comparison of Equation (10) with EC 2 at the service stage for the effective moment of inertia and deflection

Beam Name	From Equation (10)		EC 2		$\Phi_{exp}/\frac{1}{r_{t,QP}}$ %	$\frac{\Delta_{s\,EC2}}{\Delta_{s(equation10)}}$ %
	Φ_{exp} x10^{-5}(mm^{-1})	Δ_s (mm)	$\frac{1}{r_{t,QP}}$ x10^{-5} mm^{-1}	Δ_s (mm)		
BWS	1.363	3.310	1.234	3.000	110.3	90.63
BWBS	1.538	3.731	1.071	2.609	143.0	69.92
BWP3-1	1.160	2.823	1.219	2.964	95.24	104.9
BWBP3-1	1.481	3.594	1.266	3.075	116.8	85.55
BWP3-2	1.956	4.735	1.237	3.006	157.5	63.48
BWBP3-2	2.068	5.005	1.235	3.002	166.7	59.98
BWP3-3	1.609	3.901	1.074	2.615	149.1	67.03
BWBP3-3	1.704	4.130	1.234	2.999	137.71	72.61
BWP4	1.684	4.081	1.253	3.045	134.0	74.61
BWBP4	1.666	4.039	1.263	3.068	131.6	75.95
BWP5	1.530	3.712	1.201	2.920	127.1	78.66
BWBP5	1.789	4.334	1.219	2.964	146.2	68.38
BWPR4	1.914	4.635	1.068	2.599	178.3	56.07
BWBPR4	1.954	4.729	1.196	2.907	162.6	61.47
BWPL3	1.649	3.997	1.308	3.177	125.8	79.48
BWBPL3	1.600	3.901	1.237	3.006	129.7	77.05
COV					+138.26%	-74.12%

TABLE 7. Comparing the experimental deflection to the calculated deflection at the service load stage using Equation (12)

Beam Name	Modified Equation (12)					
	From Equation (2)			EC 2		
	I_{eff} x10^8	Δ_s (Equation (2)) (mm)	$\frac{\Delta_{s(eq.2)}}{\Delta_{exp}}$ x100	$\frac{1}{r_{t,QP}}$ x10^5 (mm^{-1})	Δ_s EC 2 (mm)	$\frac{\Delta_{s\,EC2}}{\Delta_{s\,exp}}$ x100
BWS	2.0460	4.0580	115.90	1.6680	4.0420	115.50
BWBS	2.1780	3.5080	97.440	1.4480	3.5130	97.600
BWP3-1	2.1110	3.9970	128.90	1.6480	3.9930	128.80
BWBP3-1	2.1260	4.1470	112.00	1.7100	4.1440	112.00
BWP3-2	2.0380	4.0480	92.000	1.6720	4.0510	92.070
BWBP3-2	2.2530	4.0450	89.880	1.6690	4.0450	89.900
BWP3-3	2.2460	3.5240	97.880	1.4520	3.5220	97.850
BWBP3-3	2.2160	4.0480	98.730	1.6670	4.0410	98.560
BWP4	2.1430	4.0960	99.900	1.6940	4.1030	100.00
BWBP4	2.2100	4.1400	103.50	1.7060	4.1340	103.30
BWP5	2.2360	3.9350	109.30	1.6230	3.9340	109.20
BWBP5	2.1120	3.9930	95.070	1.6480	3.9930	95.080
BWPR4	2.0990	3.4940	85.210	1.4430	3.5010	85.400
BWBPR4	2.1720	3.9170	91.090	1.6160	3.9170	91.090
BWPL3	2.3650	4.2890	104.60	1.7670	4.2810	104.40
BWBPL3	2.2410	4.0550	101.30	1.6710	4.0500	101.20
C.O.V			1.40 %			1.30 %

3. 4. Comparison of the Modified Stiffness Equation for Wide Beams with Other Researches The forty-three broad beams accessible in the literature and used in this work were split into five groups based on the literature [1, 2, 5-7] and tabulated in Table 8 to determine the range of the revised stiffness formula for broad beams.

Table 8 compares experimental data of deflections on the service loads (60 percent of the ultimate loads) for forty-three broad beams with findings of deflections on the service load estimated using the revised stiffens Equation (12) for these broad beams.

All forty-three specimens used to assess the applicability of the modified Equation (12) were broad beams, a/d >1, simply supported beams with rectangular sections.

Table 8 summarized the analytical data of all samples. It is obvious that -11.20%, -4.530%, -11.400%, 12.600%, and -12.900% represent the coefficient of variation [COV] for Said and Elrakib [5], Mohammadyan [6], Tapan [7], Edward [1], and Adam [2], respectively as well as the 5.480% represents the average of all COV of all beams. All of the reported data in literature [2, 5-7] unless Edward [1] showed that the deflections calculated by the revised Equation (12) were too low, which means the revised Equation (12) remain a conservative formula.

This comparison validates the adjusted Equation (12) used to calculate the effective inertia moment for wide beams.

TABLE 8. A comparison of the revised stiffness equation with other studies [5-7], [1-2]

Researcher	Experimental Results of Researcher												Δ Eq. (12)	Def. %	Point - load	Failure
	Spe.	L (mm)	B (mm)	H (mm)	a (mm)	a/d	S (mm)	f_c'	ρ_l %	ρ' %	P service	Δ_s				
M. Said [5]	SB1	1750.0	700.0	250	650	3	-	29	1.72	0.29	270	**3.0**	**3.06**	**2.15**	2.0	shear
	SB2	1750.0	700.0	250	650	3	φ6-200	29	1.72	0.29	358	**3.6**	**3.57**	**-0.77**	2.0	shear
	SB3	1750.0	700.0	250	650	3	φ8-200	29	1.72	0.29	392	**5.2**	**3.76**	**-27.5**	2.0	shear

	SB4	1750.0	700.0	250	650	3	φ6-150	29	1.72	0.29	374	**4.6**	**3.66**	**-20.3**	2.0	shear
	SB5	1750.0	700.0	250	650	3	φ8-150	29	1.72	0.29	406	**4.2**	**3.84**	**-8.34**	2.0	shear
	SB6	1750.0	700.0	250	650	3	φ6-100	29	1.72	0.29	390	**3.9**	**3.75**	**-3.66**	2.0	shear
	SB7	1750.0	700.0	250	650	3	φ8-100	29	1.72	0.29	416	**4.1**	**3.90**	**-4.70**	2.0	shear
	SB8	1750.0	700.0	250	650	3	φ10-200	29	1.72	0.29	484	**5.0**	**4.29**	**-14.0**	2.0	shear
	SB9	1750.0	700.0	250	650	3	φ10-100	29	1.72	0.29	556	**6.2**	**4.71**	**-23.9**	2.0	shear
COV														**-11.20**		
S. E. M. [6]	WB-1	1820.0	751	251	551	2.60	-	28	1.420	0.080	241.0	**1.10**	**1.210**	**10.60**	1.0	shear
	WB-2	1820.0	751	251	551	2.60	φ10-150	28	1.420	0.080	362.0	**2.20**	**1.820**	**-17.20**	1.0	shear
	WB-3	1820.0	751	251	551	2.60	804-H	28	1.420	0.080	304.0	**1.70**	**1.530**	**-9.860**	1.0	shear
	WB-4	1820.0	751	251	551	2.60	-	28	1.420	0.080	288.0	**1.40**	**1.450**	**3.740**	1.0	shear
	WB-5	1820.0	751	251	551	2.60	φ11-150	28	1.420	0.080	349.0	**2.10**	**1.970**	**-5.720**	1.0	shear
	WB-6	1820.0	751	251	551	2.60	φ11-150	28	1.420	0.080	381.0	**2.10**	**1.910**	**-8.800**	1.0	shear
COV														**-4.530**		
M. T. [7]	KD--1	2250.0	500.0	251	1126	4.90	φ8-300a	38	0.360	0.2	71.0	**4.0**	**3.38**	**-15.00**	1.0	shear
	KD--2	2250.0	500.0	251	1126	4.90	φ8-300b	38	0.360	0.2	60.0	**3.0**	**3.07**	**2.990**	1.0	shear
	KD--3	2250.0	500.0	251	1126	4.90	φ8-300c	38	0.360	0.2	74.0	**4.0**	**3.5**	**-12.30**	1.0	shear
	ND--1	2250.0	500.0	251	1126	4.90	φ8-200a	38	0.360	0.2	103	**5.0**	**4.38**	**-12.60**	1.0	shear
	ND--2	2250.0	500.0	251	1126	4.90	φ8-200b	38	0.360	0.2	94.0	**5.0**	**4.12**	**-17.30**	1.0	shear
	ND--3	2250.0	500.0	251	1126	4.90	φ8-200c	38	0.360	0.2	132	**6.0**	**5.16**	**-14.00**	1.0	shear
COV														**-11.40**		
E. G. [1]	AT-250A	2601	251	468	1301	2.96	--	37.8	0.92	--	138	**1.60**	**1.38**	**-13.90**	1.0	shear
	AT-250B	2601	253	470	1301	2.96	--	38.6	0.91	--	135	**1.30**	**1.35**	**3.680**	1.0	shear
	AT-1000A	2601	1003	470	1301	2.96	--	39.1	0.92	0.2	566	**2.50**	**1.93**	**-23.00**	1.0	shear
	AT-1000B	2601	1003	471	1301	2.96	--	37.8	0.92	0.2	529	**2.10**	**1.86**	**-11.50**	1.0	shear
	AT-3000	2601	3006	471	1301	2.96	--	40.5	0.92	0.2	1539	**2.20**	**1.86**	**-15.80**	1.0	shear
	AT--3A	2081	698	338	1041	3.38	--	37.4	0.94	--	286	**1.40**	**2.09**	**49.00**	1.0	shear
	AT--3B	2081	701	337	1041	3.38	--	37.7	0.94	0.2	305	**1.450**	**2.18**	**49.70**	1.0	shear
	AT--3C	2081	707	337	1041	3.38	--	37.2	0.94	--	311	**1.650**	**2.2**	**33.10**	1.0	shear
	AT--3D	2081	707	338	1041	3.38	--	37.2	0.94	0.2	299	**1.500**	**2.15**	**42.90**	1.0	shear
COV														**12.60**		
Ada [2]	AW-2	3701	1173	592	1851	3.66	φ15-300E	39.4	1.680	0.050	492	**4.0**	**2.98**	**-25.10**	1.0	shear
	AW-3	3701	1166	594	1851	3.66	φ15-300I	37.3	1.690	0.050	503	**5.1**	**3.05**	**-39.80**	1.0	shear
	AW-4	3701	1169	591	1851	3.66	--	39.8	1.690	0.080	436	**2.0**	**2.72**	**36.50**	1.0	shear
	AW-5	3701	1171	591	1851	3.66	φ15-300D	34.7	1.670	0.100	579	**3.0**	**3.37**	**12.80**	1.0	shear
	AW-6	3701	1170	594	1851	3.66	φ15-300E	43.8	1.680	--	506	**4.0**	**3.00**	**-24.70**	1.0	shear
	AW-7	3701	1171	592	1851	3.66	φ15-300D	35.9	1.670	0.100	645	**3.5**	**3.63**	**4.220**	1.0	shear
	AW-8	3701	1169	592	1851	3.66	--	39.5	1.690	0.100	481	**1.5**	**2.90**	**94.10**	1.0	shear
	AX-1	2081	704	340	1851	3.66	φ10-300E	42.0	1.720	0.050	277	**7.0**	**2.91**	**-58.20**	1.0	shear
	AX-2	2081	704	337	1851	3.66	φ4-300E	42.0	1.740	0.050	205	**7.5**	**2.38**	**-68.00**	1.0	shear
	AX-3	2081	708	336	1851	3.66	φ6-300D	42.0	1.740	0.080	272	**5.0**	**2.86**	**-42.40**	1.0	shear

	AX-4	2081	699	336	1851	3.66	φ8-300D	42.0	1.760	0.10	251	**3.0**	**2.70**	**-9.530**	1.0	shear
	AX-5	2081	698	336	1851	3.66	φ10-300	41.0	1.770	0.10	218	**5.5**	**2.47**	**-54.80**	1.0	shear
	AX-6	2081	704	339	1851	3.66	--	41.0	1.730	--	171	**2.0**	**2.12**	**6.980**	1.0	shear
COV														**-12.90**		
							Cumulative COV							**-5.480**		

E: Just Externally—legs.
I: Just Internally--legs
D: Both Externally, and Internally legs

4. CONCLUSIONS

1. Except for one specimen, there is not a big difference between the measured crack loads of the rest, and the difference does not go above 20% for the rest. This is because concrete and longitudinal reinforcing use the same properties.
2. By replacing the shear steel plate (with a round hole) with shear reinforcement (stirrups), there was only a 5% difference in yield load and ultimate load. Yield and ultimate loads for the rectangular opening were about 7.5% and 13.6% different. When bubbles are used, the yield load and ultimate load of a shear steel plate don't change much, but the yield load and ultimate load of a stirrup specimen go down by 10% and 14%, respectively.
3. When matched with experimental data from five different researchers, a new equation is projected to calculate the deflection in a RC broad beam based on the revised effective inertia moment, with a coefficient of variations of 5.48 percent.
4. Deflection at yield and ultimate load were both raised by an average of 20% and 28% when the shear steel plate was used in place of the stirrups. The 10% increase in deflection seen with the use of the current bubbles for the identical specimens is significant.
5. Using bubbles resulted in a 4.7% average reduction in sample weight and switching to shear steel plate from reinforcing steel of stirrups resulted in further reductions of 2.30%, 1.30%, and 1.0% for thicknesses of 3.0, 4.0, and 5.0mm, respectively.

5. REFERENCES

1. Sherwood, E.G., Lubell, A.S., Bentz, E.C. and Collins, M.P., "One-way shear strength of thick slabs and wide beams", ***ACI Structural Journal***, Vol. 103, No. 6, (2006), 794.
2. Lubell, A.S., Bentz, E.C. and Collins, M.P., "Shear reinforcement spacing in wide members", ***ACI Structural Journal***, Vol. 106, No. 2, (2009).
3. ACI, *Building code requirements for structural concrete and commentary*. 2011.
4. Hanafy, M.M., Mohamed, H.M. and Yehia, N.A., "On the contribution of shear reinforcement in shear strength of shallow wide beams", ***Life Science Journal***, Vol. 9, No. 3, (2012), 484-498.
5. Said, M. and Elrakib, T., "Enhancement of shear strength and ductility for reinforced concrete wide beams due to web reinforcement", ***Hbrc Journal***, Vol. 9, No. 3, (2013), 235-242. https://doi.org/10.1016/j.hbrcj.2013.05.011
6. Mohammadyan-Yasouj, S.E., Marsono, A.K., Abdullah, R. and Moghadasi, M., "Wide beam shear behavior with diverse types of reinforcement", ***ACI Structural Journal***, Vol. 112, No. 2, (2015), 199-208.
7. Tapan, M., "Structural response of reinforced concrete wide beams reinforced with lattice girders", ***Iranian Journal of Science and Technology. Transactions of Civil Engineering***, Vol. 38, No. C2, (2014), 337.
8. Ibrahim, A.M., Mansor, A.A., Salman, W.D. and Hamood, M.J., "Strength and ductility of bubbled wide reinforced concrete beams with diverse types of shear steel plates", ***International Journal of Engineering & Technology***, Vol. 7, No. 4.20, (2018), 502-506.
9. Eklou, R.J., Yani, M.B., Saifullah, H.A., Sangadji, S. and Kristiawan, S.A., "Experimental study: Shear behaviour of reinforced concrete beams using steel plate strips as shear reinforcement", in IOP Conference Series: Materials Science and Engineering, IOP Publishing. Vol. 1144, (2021), 012040.
10. Hamoda, A., Ahmed, M. and Sennah, K., "Experimental and numerical investigations of the effectiveness of engineered cementitious composites and stainless steel plates in shear strengthening of reinforced concrete beams", ***Structural Concrete***, (2022).
11. Mohamed, N., Elrawaff, B., Abdul Samad, A.A. and Alferjani, M., "Experimental and theoretical investigation on shear strengthening of rc precraced continuous t-beams using cfrp strips", ***International Journal of Engineering, Transactions B: Applications***, Vol. 28, No. 5, (2015), 671-676. doi: 10.5829/idosi.ije.2015.28.05b.04.
12. Ilbegyan, S., Ranjbar, M. and Abdollahi, S.M., "Shear capacity of reinforced concrete flat slabs made with high-strength concrete: A numerical study of the effect of size, location, and shape of the opening", ***International Journal of Engineering, Transactions B: Applications***, Vol. 30, No. 2, (2017), 162-171. doi: 10.5829/idosi.ije.2017.30.02b.02.
13. Rahmani, I., Maleki, A. and Lotfollahi-Yaghin, M.A., "A laboratory study on the flexural and shear behavior of rc beams retrofitted with steel fiber-reinforced self-compacting concrete jacket", ***Iranian Journal of Science and Technology, Transactions of Civil Engineering***, Vol. 45, No. 4, (2021), 2359-2375. doi: 10.1007/s40996-020-00547-x.
14. Faez, A., Sayari, A. and Manei, S., "Retrofitting of rc beams using reinforced self-compacting concrete jackets containing aluminum oxide nanoparticles", ***International Journal of Engineering, Transactions B: Applications***, Vol. 34, No. 5, (2021), 1195-1212. doi: 10.5829/ije.2021.34.05b.13.
15. Mohsenzadeh, S., Maleki, A. and Lotfollahi-Yaghin, M.A., "Strengthening of rc beams using scc jacket consisting of glass fiber and fiber-silica fume composite gel", ***International Journal of Engineering, Transactions B: Applications***, Vol. 34, No. 8, (2021), 1923-1939. doi: 10.5829/ije.2021.34.08b.14.

16. Aydin, E., Ozturk, B. and Duzel, E., "Rehabilitation of planar building structures using steel diagonal braces and dampers", ***rehabilitation***, Vol. 16, No. 17, (2012), 18.
17. Aydin, E., Öztürk, B., Çetin, H. and Gasir, M., "Strengthening plane frames with steel plates", (2018).
18. Johnston, F.P.B.E.R., "Jr. John t. De wolf, "Mechanics of Materials, Lecture Notes: J. Walt Oler Texas Tech University, (2009).
19. MacGregor, J.G., Wight, J.K., Teng, S. and Irawan, P., "Reinforced concrete: Mechanics and design, Prentice Hall New Jersey, Vol. 3, (1997).
20. Mohammad, M., Mohd, Z.B.J., Ali, A.M., Shatirah, A., Mohamed, J., Rafiepour, N., Mohammadhassani, A., Sinaei, H., Heydar, R.E. and Ghanbari, F., "Bending stiffness and neutral axis depth variation of high strength concrete beams in seismic hazardous areas: Experimental investigation", ***International Journal of Physical Sciences***, Vol. 6, No. 3, (2011), 482-494.

Persian Abstract

چکیده

رکاب معمولی به طور گسترده در تمام تیرهای بتنی به عنوان تقویت کننده برشی برای جلوگیری از شکست برشی که به طور ناگهانی و غیرمنتظره بدون هشدار قبلی رخ می دهد، استفاده می شود. کشف نوع دیگری از رکاب و ایجاد یک فرمول جدید برای محاسبه انحراف، چالش بزرگی است. این مقاله یک مطالعه تجربی را ارائه می‌کند که فرمول جدیدی را برای محاسبه انحراف در تیرهای بتنی تقویت‌شده با صفحات فولادی برشی به عنوان رکاب پیش‌بینی می‌کند. کار آزمایشی ایجاد شد و شامل ۱۶ تیر بتن مسلح عریض با ابعاد x560x1800۲۱۶ میلی متر است. به جای رکاب های تقویت کننده معمولی، صفحات فولادی با ضخامت های ۳.۰، ٤.۰ و ۵.۰ میلی متر در ابعاد طولی و عرضی و برای نیمی از نمونه ها، حباب های گرد PVC بازیافتی به عنوان متغیرهای مورد بررسی در این مطالعه استفاده شد. علاوه بر این، متغیرها شامل بررسی فرم بازشوی صفحات فولادی برشی با فواصل متفاوت بین آنها می باشد. برای محاسبه انحراف پرتوهای عریض، فرمول جدیدی برای ممان اینرسی موثر پیشنهاد شده است و با ضریب تغییرات ۵.٤۸ درصد، تطابق عالی را برای چندین بررسی به دست می‌دهد. فرمول های محاسبه حداکثر انحراف با استفاده از ACI 318M-14 و EC 2 ایجاد شده است.